The Co + CO Reaction: Infrared Matrix Isolation Study and Density Functional Calculations

Benoît Tremblay,* Mohammad Esmaïl Alikhani, and Laurent Manceron

L.A.D.I.R./Spectrochimie Moléculaire, U.M.R. 7075, Université Pierre et Marie Curie, Case Courrier 49, 4 Place Jussieu, 75252 Paris, Cedex 05, France

Received: June 26, 2001; In Final Form: September 28, 2001

The Co + CO reaction argon has been reinvestigated using deposition of ground-state reagents in solid argon. The Co + CO reaction products observed without activation energy are Co_2CO, a van der Waals Co···CO complex, and the higher carbonyl species $Co(CO)_x$. Infrared radiation at approximately 3000 cm^{-1}, to promote Co into the first excited-state b ^4F ($3d^84s^1$ configuration), converts the van der Waals complex to the chemically bound, most stable carbonyl form CoCO. A second irradiation with an approximately 580 nm wavelength (17000 cm^{-1}) reconverts the chemically bound CoCO ($^2\Delta$) state into the Co···CO van der Waals ($^4\Phi$) state. The photoprocess is fully reversible. Isotopic data on ν_1, ν_2, ν_3, $2\nu_1$, $\nu_1 + \nu_2$, and $\nu_1 + \nu_3$ have been measured in the near- and far-infrared regions for the carbonyl form. This enables a complete harmonic force-field calculation based on a linear geometry, in agreement with all theoretical predictions. DFT calculations of the geometrical and electronic properties of CoCO complexes from the Co + CO reaction are also presented and compared to the experimental values. Reaction mechanisms are proposed and comparisons with bond force constants of NiCO and CuCO are also presented.

Introduction

The important role played by the CO molecule in chemisorption processes and catalysis or as ligand in transition metal complexes has stimulated both theoretical and experimental studies on model compounds. For this reason, the matrix isolation technique has been applied early to the characterization of simple, unsaturated binary $Co(CO)_x$ ($x = 1-4$) cobalt carbonyls. Concerning the most elementary of all, the cobalt monocarbonyl CoCO species, isolation was first claimed by Hanlan and co-workers[1] by reaction of ground-state Co atoms and carbon monoxide molecules. CoCO was then identified as the carrier of an IR absorption near 1953 cm^{-1} in solid argon. Interestingly, no ESR activity was reported for this species in this study. Recently, Zhou and Andrews reinvestigated the reaction between laser-ablated Co atoms and carbon monoxide in argon and neon matrixes.[2,3] In argon, these authors reassigned the IR band near 1953 cm^{-1} to a higher order $Co_x(CO)_y$ species, and assigned a band at 1957.3 cm^{-1}, with notably different isotopic effects, to the monocobalt monocarbonyl molecule CoCO. This result would then indicate that the chemically bound carbonyl species was not observed in the previous study, which in turn implies that the experimental conditions specific to the laser-ablation experiments are necessary for the observation of CoCO; that is, excited-state reactions and photochemistry might play a role in the reaction. In any case, due to the low reaction yield, presently available vibrational data are restricted to the strongly absorbing ν_1 carbonyl stretching fundamental. This study presents a reinvestigation of the Co + CO reaction in solid argon with a double goal: (i) assess the reactivity of Co in the ground state (^4F, $3d^74s^2$ configuration) with respect to CO or the available reaction channels involving the first excited states and (ii) complete our knowledge of the ground-state vibrational frequencies of CoCO, in particular the low-frequency stretching and bending modes in the far-infrared.

Nickel and copper monocarbonyls have already been the subject of complete infrared studies by our group,[4,5] and we present now the results for CoCO. In comparison with the NiCO and CuCO systems, CoCO has been the subject of fewer number of theoretical studies.[3,6−8] In contrast with CuCO, also predicted to have a doublet ground state with a bent geometry, CoCO is predicted in each of these studies to have a linear ground state structure. All the studies on CoCO have used the density functional approach, but with different functionals and basis sets. All these studies present relatively similar predictions on the upper frequency, CO stretching mode (less than 3% difference, see DFT Calculations and Reaction Mechanism), but differ significantly on the energies of the lower frequency metal−ligand vibrations. These are more sensitive markers of the description of the metal−ligand interaction as the associated normal coordinate follows more closely the reaction coordinate. Such experimental results on these molecules are thus interesting to test the validity of these calculations.

We report here the frequencies of the Co−CO stretching and bending vibrations ν_1, ν_3 and ν_2, for several isotopic species (the $^{12}C^{16}O$, $^{13}C^{16}O$, $^{12}C^{18}O$, and $^{13}C^{18}O$ isotopic species for CO). New isotopic data on the CO stretching vibration and observations of overtone and binary combination levels in the near-infrared are reported. DFT calculations of the geometrical and electronic properties of CoCO complexes from the Co + CO reaction are also presented and compared to the experimental values. A reaction mechanism is proposed and comparisons with bond force constants of NiCO and CuCO are also presented.

Experimental Section

Experimental procedures and methods were the same as those used in refs 4 and 5. The CoCO molecules were prepared by

* To whom correspondence should be addressed. Fax: 33-1-44273021. E-mail: tremblay@ccr.jussieu.fr.

10.1021/jp012422g CCC: $20.00
Published on Web 11/28/2001

co-condensing cobalt vapor and dilute CO−Ar mixtures (0.1−2% CO in Ar) onto a flat, highly polished, Ni-plated copper mirror maintained at ca. 10 K using a closed-cycle cryogenerator, situated in a stainless steel cell evacuated at a base pressure less than 5×10^{-7} mbar, before refrigeration of the sample holder. A tungsten filament, mounted in a furnace assembly and wetted with cobalt (Alpha Inorganics, 99.9965%), was heated from 1200 to 1400 °C to generate the Co vapor. The metal deposition rate was carefully monitored with the aid of a quartz microbalance and was typically of the order of about 0.2−1.2 μg/min.

High-purity argon (Prodair; 99.995%) and carbon monoxide (Matheson; 99.5%), ^{13}CO (CEA, Saclay, France; 99% ^{13}CO including 8% $^{13}C^{18}O$), $^{12}C^{18}O$ (MSD; 98% ^{18}O), or $^{13}C^{18}O$ (CEA, Sarclay, France; 60%$^{13}C^{16}O$ + 40% $^{13}C^{18}O$) were used to prepare the CO−Ar mixtures after removing condensable impurities with a liquid nitrogen trap.

In general, after deposition times varied between 20 and 90 min, infrared spectra of the resulting sample were recorded in the transmission−reflection mode between 5000 and 70 cm^{-1} using a Bruker 120 FTIR spectrometer and suitable combinations of CaF_2/Si, KBr/Ge, or 6 μm Mylar beam splitters with either liquid N_2-cooled InSb or narrow band HgCdTe photodiodes or a liquid He-cooled Si−B bolometer, fitted with cooled band-pass filters. The resolution was varied between 0.1 and 0.5 cm^{-1}. Bare mirror backgrounds, recorded at 10 K from 5000 to 70 cm^{-1} prior to sample deposition, were used as references in processing the sample spectra. Also, absorption spectra in the near-, mid-, and far-infrared were collected on the *same* samples through CaF_2, CsI, or polyethylene windows mounted on a rotatable flange separating the interferometer vacuum (10^{-2} mbar) from that of the cryostatic cell (10^{-7} mbar). The spectra were subsequently subjected to baseline correction to compensate for infrared light scattering and interference patterns.

The sample was next irradiated, typically between 1 and 2 h, using a globar lamp and a combination of a 3200 cm^{-1} low-pass filter with a 2750 cm^{-1} high-pass filter. It was found that the subject of study, the CoCO molecule, could be selectively formed by irradiation at this wavelength. A second irradiation, for approximately 30 min, using a 200 W mercury−xenon high-pressure arc lamp and an interference filter centered on the Hg emission line near 580 nm (17000 cm^{-1}), destroyed the CoCO molecule. Infrared spectra of the photolyzed samples were recorded between 5000 and 70 cm^{-1} as outlined above.

Experimental Results

Co vapor was co-condensed with relatively dilute mixtures of CO in argon (0.5−2/100) at 10 K to favor formation of monocarbonyls, Co_xCO. In the CO stretching region, the only range covered in the earlier studies, the products are very strongly absorbing and the reactant concentrations can be varied over 2 orders of magnitude. Even for a 1% CO/Ar samples, five absorptions can be detected in this region (Figure 1): a weak one at 2133.7 cm^{-1} on the low-frequency side of the very strong band of unreacted CO, two sharper ones at 1957.5 cm^{-1} (1 cm^{-1} full width at half-maximum, fwhm) and 1953.3 cm^{-1} (1.4 cm^{-1} fwhm), and two broader ones at 1921.6 and 1983.6 cm^{-1}. The latter two were previously assigned by Hanlan et al. to $Co(CO)_2$ and $Co(CO)_3$, respectively[1]. However, this group assigned the band near 1953 cm^{-1} to the CoCO molecule. In the recent work of Zhou and Andrews,[2] a new band at 1957.3 cm^{-1} was assigned to CoCO, and the band at 1953.3 cm^{-1} reassigned to a $Co_x(CO)_y$ species.

After studying the concentration dependence of the bands at 2133.7, 1957.5 and 1953.3 cm^{-1} over a very wide range, it

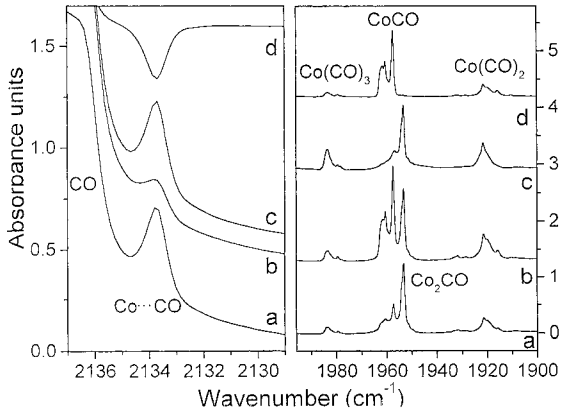

Figure 1. Infrared spectra of van der Waals *Co···CO* complex (near the diatomics CO stretching region) and Co_2CO, CoCO, $Co(CO)_2$, and $Co(CO)_3$ molecules in the C−O stretching region with Co/CO/Ar molar ratio of 0.25/2/100. (a) after deposition, (b) after irradiation at approximately 3000 cm^{-1}, (c) after irradiation at 580 nm, and (d) difference between spectrum b and a.

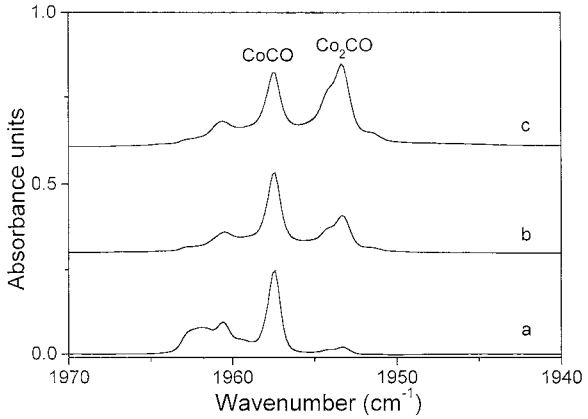

Figure 2. Infrared spectra of CoCO and Co_2CO molecules in the CO stretching region: a cobalt concentration study with a 1% CO/Ar mixture. From bottom to top: Co/CO/Ar = 0.05/1/100; Co/CO/Ar = 0.1/1/100, absorbance scale × 0.5; Co/CO/Ar = 0.25/1/100, absorbance scale × 0.2.

appears that the three bands have the same linear dependence with respect to CO concentration. Varying the cobalt concentration, the bands at 2133.7 and 1957.5 cm^{-1} have a similar linear dependence, while the band at 1953.3 cm^{-1} has a quadratic dependence (Figure 2). With these considerations, we can assign this latter band to the $Co_2(CO)$ species, the band at 1957.5 cm^{-1} to the CoCO molecule and the band at 2133.7 cm^{-1}, which is 4.7 cm^{-1} redshifted with respect to the unreacted CO band, to a molecular complex with one cobalt atom and one CO molecule, not observed previously. Data on these two species are presented in Table 1.

The experiments were repeated using isotopically labeled CO, more specifically $^{13}C^{16}O$, $^{12}C^{18}O$, and $^{13}C^{18}O$. The results of the isotopic study are presented in Figures 3−5 and Table 1. In the CO stretching region (Figure 3) the main bands at 1957.5 and 2133.7 cm^{-1} shift to 1910.3, 1917.4, and 1869.0 cm^{-1}and 2086.8, 2082.8, and 2034.6 cm^{-1} when $^{12}C^{16}O$ is replaced by $^{13}C^{16}O$, $^{12}C^{18}O$, and $^{13}C^{18}O$, respectively. Similarly, in the far IR region, isotopic substitution causes both the bands at 579.2 and 424.9 cm^{-1} to shift (Figure 4). More specifically, the band at 579.2 cm^{-1} shifts to 573.9 and 564.2 cm^{-1} upon replacing $^{12}C^{16}O$ by $^{13}C^{16}O$ and $^{12}C^{18}O$, respectively, while the absorption at 424.9 cm^{-1} shifts to 411.7 and 421.2 cm^{-1}, with these same precursors. In an experiment run with a mixture of $^{13}C^{16}O$ and $^{13}C^{18}O$, the $Co^{13}C^{18}O$ counterparts appear at 559.7 and 407.9

TABLE 1: Vibrational Frequencies[a] and Relative Intensities of the IR Absorption Bands Observed for Various Species of CoCO Molecule and Co···CO van der Waals Complex

$Co^{12}C^{16}O$		$Co^{13}C^{16}O$	$Co^{12}C^{18}O$	$Co^{13}C^{18}O$	assignment
3900.5		3803.8	3818.3	3716.1	$2\nu_1$
3899.3	[0.0165][b]	3801.5	3811.9		
3897.2		3797.7			
3890.9					
2544.9		2484.1	2481.1	2428.3	$\nu_1 + \nu_3$
2542.7	[0.0020]	2482.7	2479.7	2427	
2536.3					
2534.9					
2377.2		2317.4	no[c]	no	$\nu_1 + \nu_2$
2374.5	[0.0004]	2314.9			
2373.6					
2133.7	[0.0720]	2086.8	2082.8	2034.6	ν_{CO} in Co···CO
1961.8		1913.3	1920.4	1873.1	ν_1
1960.6	[1]	1910.3	1917.4	1871.9	
1957.5				1869.0	
583.8		573.9	564.2	565	ν_3
580.1	[0.0025]			564	
579.2				559.7	
424.9		411.7	421.2	407.9	ν_2
421.0	[0.0093]	409.4	418.6	405.5	
421.0		408.1	417.2	404.2	
420.1					

[a] Vibrational frequencies in cm^{-1}. The values quoted are within $\pm$ 0.1 cm^{-1}, except for the integer values. The value of the main site is underlined. [b] Relative IR intensities with respect to ν_1. The ν_1 absolute intensity is estimated to be 860 $\pm$ 90 km/mol. [c] Not observed.

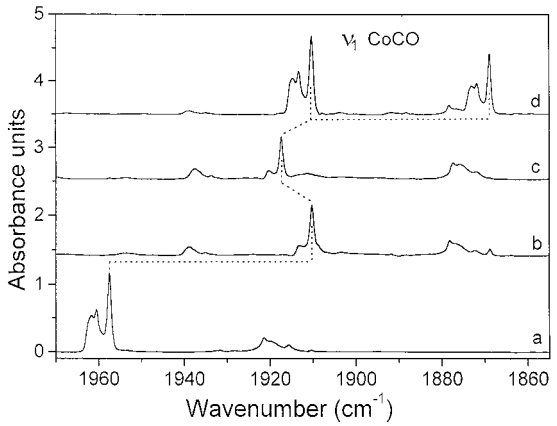

Figure 3. Infrared difference spectra of cobalt monocarbonyl in the CO stretching region for various isotopic precursors. (a) Co + CO, (b) Co + ^{13}CO, (c) Co + $C^{18}O$, and (d) Co + ($^{13}C^{16}O$+$^{13}C^{18}O$). The ^{13}CO sample contains about 8% $^{13}C^{18}O$ as isotopic impurity. In all samples the Co/CO/Ar molar ratios are approximately the same: 0.05/2/100.

cm^{-1} in the far-infrared (top spectra of Figure 4). The feature at 3890.9 cm^{-1}, at about twice the frequency of the CO stretching, shifts to 3797.7, 3811.9, and 3716.1 cm^{-1} when $^{13}C^{16}O$, $^{12}C^{18}O$, and a mixture of $^{13}C^{16}O$ and $^{13}C^{18}O$ are substituted for $^{12}C^{16}O$ (Figure 5). The feature at 2534.9 cm^{-1}, consistent with the combination of the CO stretching mode at 1957.5 cm^{-1} and the mode at 579.2 cm^{-1}, shifts to 2482.7, 2479.7, and 2427 cm^{-1} when $^{12}C^{16}O$ is replaced by $^{13}C^{16}O$, $^{12}C^{18}O$, and a mixture of $^{13}C^{16}O$ and $^{13}C^{18}O$, respectively (Figure 5).

Finally, the feature at 2377.2 cm^{-1}, consistent with the combination of the CO stretching mode at 1957.5 cm^{-1} and the mode at 424.9 cm^{-1}, shifts to 2317.4 cm^{-1} when $^{12}C^{16}O$ is

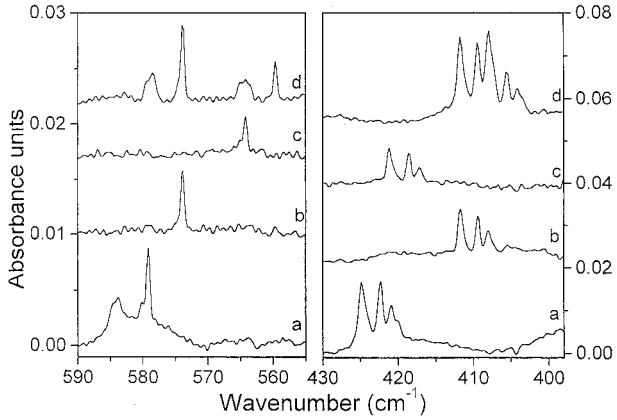

Figure 4. Infrared difference spectra of cobalt monocarbonyl in the low-frequency stretching mode (ν_3) and the bending mode (ν_2) regions for various isotopic precursors. (a) Co + CO, (b) Co + ^{13}CO, (c) Co + $C^{18}O$, and (d) Co + ($^{13}C^{16}O$+$^{13}C^{18}O$). The ^{13}CO sample contains about 8% $^{13}C^{18}O$ as isotopic impurity

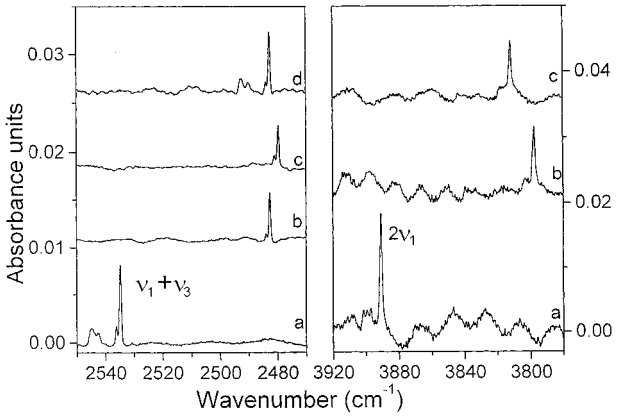

Figure 5. Infrared difference spectra of cobalt monocarbonyl in the CO stretching overtone region and in the $\nu_1 + \nu_3$ combination region for various isotopic precursors. (a) Co + CO, (b) Co + ^{13}CO, (c) Co + $C^{18}O$, and (d) Co + ($^{13}C^{16}O$+$^{13}C^{18}O$).

replaced by $^{13}C^{16}O$. With the $^{12}C^{18}O$ isotope, the counterpart of the band at 2377.2 cm^{-1} has not been observed because this band is very near the strong absorption of the CO_2 molecule around 2340 cm^{-1}. With the $^{13}C^{16}O$ + $^{13}C^{18}O$ mixture, the counterpart of the band at 2377.2 cm^{-1} has not been observed because the mixture used contained only 40% of $^{13}C^{18}O$.

The sample was next irradiated using a globar lamp and a 3200−2750 cm^{-1} band-pass filter. It was found that the CoCO molecule selectively grew by irradiation in this domain, while the molecular complex at 2133.7 cm^{-1} is partially destroyed. More precisely, after irradiation, three bands grow at 1961.8, 1960.6, and 1957.5 cm^{-1} (Figure 1). These bands can thus be assigned to the stretching vibration ν_1 of the CoCO molecule present in different trapping sites in the argon matrix. The existence of several, slightly different trapping sites will be confirmed on the other fundamental, harmonic, and combination transitions of this molecule (see Table 1). A second irradiation, for approximately 30 min, using a 200 W mercury−xenon high-pressure arc lamp and an interference filter centered at 580 nm destroyed the CoCO molecule, and the 2133.7 cm^{-1} band comes back to its initial intensity (Figure 1). From this we can infer that these two bands correspond to two different isomeric forms of the same system. Also, the isotopic shifts for the 2133.7 cm^{-1} band when $^{12}C^{16}O$ is replaced by $^{13}C^{16}O$, $^{12}C^{18}O$, and $^{13}C^{18}O$ (−46.9, −50.9, and −99.1 cm^{-1}) are very similar, within experimental errors, in comparison with the isotopic shifts for

TABLE 2: Comparison of the Experimental Vibrational Frequencies of CoCO ($^2\Delta$) with the Harmonic Frequencies Calculated by a Number of DFT Calculations

	experimental	DFT calculations				
Σ^+ C−O stretch						
ν_1[a]	1957.5 (860)[b]					
ω_1	1989	1971 (754)[c]	1980.5 (697)	2052 (585)	2020	1979 (686)
Π symmetry bending						
ν_2	424.9 (8.0)					
ω_2		370 (10)	358.0 (11)	320 (13)	356	n.c.[d]
Σ^+ Co−C stretch						
ν_3	579.2 (2.2)					
ω_3		609 (6)	598.9 (4)	645 (2)	513	n.c.
R_{C-O} (Å)		1.170	1.170	1.171	1.150	1.170
R_{Co-C} (Å)		1.673	1.682	1.645	1.709	1.667
dissociation energy[e]		45	n.c.	30	26.8	57.5
ref	this work	this work	3	6	7	8

[a] Vibrational frequencies in cm^{-1}. [b] Estimated absolute IR intensities (±10%, in km/mol, see text). [c] Calculated absolute IR intensities. [d] Not calculated. [e] The definition of the dissociation energy (in kcal/mol) is not the same in all the theoretical works.

the band of unreacted CO (−47.1, −51.0, and −99.4 cm^{-1}). We can conclude that the band at 2133.7 cm^{-1} corresponds to the CO vibration of a very weakly perturbed CO moiety, thus attributable to a metastable state of the Co···CO system in which no chemical bonds takes place, held at most by van der Waals interactions. It is noteworthy that the efficient energy to induce photoconversion corresponds to that necessary for the $a^4F \rightarrow b^4F$ atomic transition.[9]

Several new absorptions appeared both in the far- (Figure 4) and near-infrared regions (Figure 5). Among these, five absorptions near 425, 579, 2377, 2535, and 3891 cm^{-1} presented a relative intensity dependence proportional to either cobalt or carbon monoxide concentrations and behaved, upon the two irradiations, similarly to the strong ν_1 band at 1957.5 cm^{-1}. This shows that these absorptions belong to the same species, i.e., CoCO.

The IR intensity measurements required here special attention, as the subject of study present both very strong and very weak absorptions, and in different spectral domains. Care was taken, first, to make measurements on the *same* samples in the various spectral ranges, second, to repeat these measures on optically thin and thick samples in order to avoid large photometric errors and, last, to use band decomposition procedure to estimate relative intensities for partially overlapping bands. The values reported in Table 1 are relative intensities normalized with respect to the strongest fundamental, at 1957.5 cm^{-1}. Also, an estimate of the absolute intensities was possible here as it is possible to follow, with the irradiations, the growth of CoCO molecule correlated with the disappearance of the parent Co···CO. A 14 ± 1.5 integrated intensity ratio can be derived between the ν_1 CO stretching vibration of CoCO and the CO stretching fundamental in Co···CO, assuming that the CO vibration infrared intensity of the Co···CO is the same as that in the CO diatomic molecule. This yields an estimate of 860 ± 90 km/mol for this very strong band, from known integrated intensities.[10]

DFT Calculations and Reaction Mechanism. All the articles on CoCO have used the density functional approach (DFT), but with different functionals and basis sets. All these studies present relatively similar predictions on the upper frequency, CO stretching mode (less than 3% difference, see Table 2), but differ significantly on the energies of the lower frequency metal−ligand vibrations and the prevision of the dissociation energy. These results show the sensitivity of this difficult system to the functional and/or basis sets employed. The main motivation of the present calculations (with the same method (DFT)) is to understand the energetics and reaction mechanisms between a cobalt atom and a CO molecule. We have studied the reactivity of the cobalt atom in different excited states and we have calculated the CoCO molecule in different states.

All calculations were carried out using the Gaussian 98 quantum chemical package.[11] A pure DFT method containing the gradient corrections of Becke[12] for exchange and of Perdew−Wang[13] for correlation were used for the exchange−correlation energy. This functional has been called BPW91. The 6-311 + G(2d) extended basis set of Pople et al.[14,15] has been used for oxygen and carbon. For CO, the basis set of Schaefer et al.[16] with triple-ζ quality in the valence region (17s10p6d)/[6s3p3d] was chosen. Reproducing the correct ordering and separation of electronic states in first-row transition metal atoms is a very difficult task in electronic structure theory. For instance, in refs 6 and 7, using similar functionals but less extended basis set, the correct ordering of the two first electronic states of the cobalt atom was not reproduced. A $3d^84s^1$ ground state was thus predicted and the procedure had to be modified before being able to assist the data interpretation. We believe that it is a fundamental preliminary step before obtaining a semiquantitative evaluation of energy level separation and bond dissociation energy of the metal−carbonyl molecule. The experimental values for the energy separation between the ^4F ($3d^74s^2$) ground state and the ^4F ($3d^84s^1$) and ^2F ($3d^84s^1$) excited states of the Co atom are 3483 and 7442 cm^{-1}, respectively.[9] Therefore, we used a basis set large enough to find the correct level ordering and energy separation. The computed electronic configuration of the first two excited states [b^4F ($3d^84s^1$)] and [a^2F ($3d^84s^1$)] are here correct and their energy difference is in good agreement with the experimental value (4542 vs 3959 cm^{-1}). Because both these excited states are high in energy, the first state of CoCO accessed from ground-state Co (a^4F) is a weakly bound van der Waals complex (mostly $^4\Phi$). As stated by experimental considerations, the coordinated complex is formed after photoexcitation. DFT is not well suited for assessing the very weak binding energy for van der Waals-like interaction as for the $^4\Phi$ state. Calculations done at the MP2 level with the same basis set indicate a BSSE-corrected binding energy of less than 1 kcal/mol, i.e., at most a very weakly bound state.

The reaction of the Co atom in the first excited state ^4F ($3d^8$-$4s^1$ configuration) with CO gives the CoCO molecule in a $^4A''$ state with bent structure, and a dissociation energy of 28 kcal/mol. The molecular ground state corresponding to the CoCO molecule ($^2\Delta$) was obtained from the Co atom in the second excited state ^2F ($3d^84s^1$), with a dissociation energy of 45 kcal/mol, corrected for the zero-point energy and basis set superposition error, calculated with respect to Co (b^4F) + CO ($^1\Sigma$)

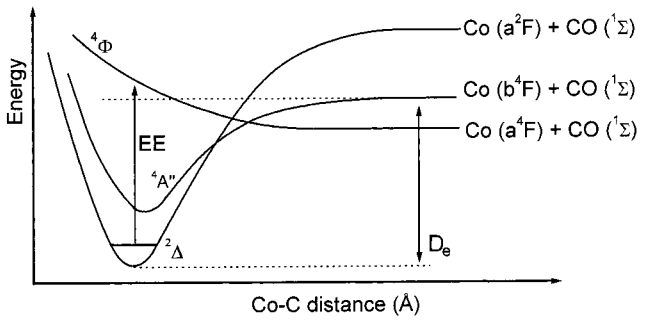

Figure 6. Schematic potential curves for the ^{4}A″ excited state and $^2\Delta$ ground state of the CoCO molecule, with the $^4\Phi$ state of the Co···CO. An experimental excitation energy (EE) with approximately 580 nm light (17000 cm^{-1}) reconverts the chemically bound CoCO in van der Waals Co···CO bound state.

fragments. The binding energy with respect to ground-state reagents will thus correspond to about −35 kcal/mol. Our calculated geometrical parameters are very similar with those reported by Swang et al.[8] At the MP2 level of theory, we have found geometrical parameters (r_{CO} =1.202 Å, r_{CoC} =1.652 Å, and D_0= 55 kcal/mol) close to those obtained with BPWP1. We should note that the predicted molecular properties for ground state CoCO do not vary much from one method to the other (MP2 and DFT), but the calculated dissociation energy depends strongly on the basis set. This is why a correct prediction of the metal atomic levels is indispensable for a reliable adiabatic binding energy estimate.

These results are schematized in Figure 6 (the potential curves are here only schematic). Also, it is important to note that the energy necessary to the promotion of an electron from 4s level to 3d level in cobalt (3483 cm^{-1}) corresponds approximately to the energy of the infrared radiation (between 3200 and 2750 cm^{-1}) required to convert the Co···CO in stable CoCO molecule. From these experimental and theoretical results, the photochemical cycle observed for the Co + CO system can be divided in four steps: (1) the interaction between a cobalt atom in the ground state and CO gives a weakly bound van der Waals complex Co···CO ($^4\Phi$); (2) electronic excitation of this complex in the infrared between 3200 and 2750 cm^{-1} causes the promotion of the cobalt atom in b^{4}F ($3d^8 4s^1$) state, which reacts with CO to form the CoCO molecule in an intermediate ^{4}A″ state; (3) the ^{4}A″ excited-state potential energy surface crosses the $^2\Delta$ ground state, and next, since the $^2\Delta$ curve is attractive after the intersystem crossing region, the CoCO molecule can hop onto the $^2\Delta$ curve which corresponds to the ground state; and last (4) a second irradiation at approximately 17 000 cm^{-1} reconverts the chemically bound CoCO in metastable (mostly $^4\Phi$) Co···CO state. The energy of the second photon which enables back-conversion in the $^4\Phi$ state places an upper limit (largely overestimated) to the dissociation energy: 49 kcal/mol. Our calculated bond dissociation energy is in line with this conclusion. When accessed through photoexcitation via the $^2\Delta$ state, the fragments should have high translational energies. In the gas phase this should lead to photodissociation, while here the presence of the matrix cage quenches the excess kinetic energy and relaxes the system back the $^4\Phi$ state.

This scheme explains the apparent discrepancy between previous metal laser ablation[2,3] and thermal effusion works.[1] The metal atoms produced by laser-ablation are not necessary in the ground state, and the species isolated in the matrix are subjected to photolysis with the laser plume during deposition, which will cause the direct appearance of the final product, bypassing the intermediate steps. The former thermal evaporation work by Hanlan et al. did not attempt photoexcitations, and the CoCO species was not formed in these experiments.

In conclusion, we can fully confirm Zhou and Andrews identification of the 1957.5 cm^{-1} band as belonging to the cobalt monocarbonyl chemically bound state but add a band at 2133.7 cm^{-1} to the same stoichiometry.

Vibrational Analysis and Harmonic Force Field Calculations. From the concentration and isotopic effects, the positions of six absorption bands belonging to CoCO have been clearly established, which means that at least three out of the six absorptions are either overtone or combination levels. Previous work[2] had assigned the band at 1957.5 cm^{-1} to the CO stretching vibration of CoCO. With arguments detailed in the preceding section, it is confirmed that this band, along with that at 1961.8 and 1960.6 cm^{-1}, belong to the trapping sites of CoCO (Table 1). For the rest of discussion we shall focus on the frequencies measured for the main site, at 1957.5 cm^{-1}, as the signals are stronger and sharper, and therefore allowing a more precise discussion of the isotope effects and of their structural implications.

For the band observed at 1957.5 cm^{-1}, assignment to the ν_1 CO stretching vibration of CoCO was straightforward, but the isotopic effects are interesting to analyze in more details. ν_1 shifts to lower frequency by 47.2 cm^{-1} when $^{13}C^{16}O$ is used, by 40.1 cm^{-1} in the case of $^{12}C^{18}O$ and by 88.5 cm^{-1} for $^{13}C^{18}O$. The ν_1 frequency for $Co^{12}C^{18}O$ is larger than that for $Co^{13}C^{16}O$ despite a smaller reduced mass for a CO isolated oscillator. This indicates a substantial vibrational coupling between the CO and CoC oscillators despite the differences in reduced masses and bond strength which must be taken into account for an accurate discussion of the molecular parameters. Appraising the difference between the $^{16}O/^{18}O$ and $^{12}C/^{13}C$ isotopic shifts for an isolated CO oscillator (+3.83 cm^{-1}) and those observed actually for the metal carbonyl molecule (−7.10 cm^{-1} for CoCO) is indeed an alternative, albeit indirect, indication of the metal−ligand bond strength. In the related NiCO species[4] in which the ν_3 metal−CO stretching mode frequency is similar (Table 5), this difference reaches 41.0−47.9 = −6.9 cm^{-1}. For CuCO,[5] with a much weaker metal−ligand interaction, this difference is +3.5 cm^{-1}, virtually that for an isolated CO oscillator, despite similar ν_1 mode frequencies (Table 5).

There is a general agreement[3,6−8] that CoCO should have $C_{\infty v}$ symmetry, thus the Co−CO deformation mode, or ν_2, would be in a symmetry class of its own. Using the Wilson's method[17] and the ground-state geometry calculated in this study, i.e., r_{CoC} = 1.673 Å and r_{CO} = 1.170 Å, we can determine the frequency shifts expected for ν_2 when $^{12}C^{16}O$ is substituted by $^{13}C^{16}O$, $^{12}C^{18}O$, and $^{13}C^{18}O$. Specifically, substitution of $^{12}C^{16}O$ by $^{13}C^{16}O$ should cause a much larger shift to lower frequencies than substitution by $^{12}C^{18}O$. This trend is observed for the band at 424.9 cm^{-1}. In fact, isotopic substitution caused the band to shift by −13.2 cm^{-1} for $Co^{13}C^{16}O$, −17.0 cm^{-1} for $Co^{13}C^{18}O$, and by only −3.7 cm^{-1} for $Co^{12}C^{18}O$. The band at 424.9 cm^{-1} must therefore be assigned to the ν_2 bending mode of CoCO. Furthermore, Table 3 contains the calculated DFT frequencies shifts upon isotopic substitutions. The calculated shifts are in excellent agreement with the experimental isotopic shifts for this assignment.

For the remaining Σ^+ symmetry fundamental, the Co−CO stretching, one would expect that substitution of $^{12}C^{16}O$ by $^{13}C^{16}O$, $^{12}C^{18}O$, and $^{13}C^{18}O$ would result in increasing shifts ($\Delta\nu$) to lower frequencies. Furthermore, it is expected that $\Delta\nu(Co^{13}C^{18}O) > \Delta\nu(Co^{12}C^{18}O) > \Delta\nu(Co^{13}C^{16}O)$. This is what is observed for the band at 579.2 cm^{-1}, and we have assigned

TABLE 3: Comparison of the Experimental and Calculated (DFT) Frequencies Shifts (cm^{-1}) for the Various Isotopic Species of CoCO

	$\Delta\nu$ ($Co^{12}C^{16}O-Co^{13}C^{16}O$)		$\Delta\nu$ ($Co^{12}C^{16}O-Co^{12}C^{18}O$)		$\Delta\nu$ ($Co^{12}C^{16}O-Co^{13}C^{18}O$)	
	exptl	DFT	exptl	DFT	exptl	DFT
$\nu_1(\Sigma^+)$	47.2	49.0	40.1	40.3	88.5	90.2
$\nu_3(\Sigma^+)$	5.3	5.8	15.0	16.3	19.5	21.2
$\nu_2(\Pi)$	13.2	11.0	3.7	4.1	17.0	15.4

TABLE 4: Comparison of the Experimental Frequencies and Calculated[a] Harmonic Frequencies (cm^{-1}) for the Various Isotopic Species of CoCO

	$Co^{12}C^{16}O$		$Co^{13}C^{16}O$		$Co^{12}C^{18}O$		$Co^{13}C^{18}O$	
	exptl	calcd	exptl	calcd	exptl	calcd	exptl	calcd
$\nu_1(\Sigma^+)$	1957.5	1957.5	1910.3	1909.5	1917.4	1917.1	1869.0	1867.7
$\nu_3(\Sigma^+)$	579.2	579.2	573.9	573.7	564.2	563.9	559.7	559.2
$\nu_2(\Pi)$	424.9	424.9	411.7	412.0	421.2	420.1	407.9	407.1

[a] The force constants giving the best fit of the experimental data are $F_{CoC} = 3.96$ mdyn $Å^{-1}$, $F_{CO} = 14.739$ mdyn $Å^{-1}$, $F_{CoC,CO} = 0.55$ mdyn $Å^{-1}$, and $F_{CoCO} = 0.4675$ mdyn Å rad^{-2}.

this band to the ν_3 stretching mode of CoCO. The results of the Table 3 are also in agreement with this assignment.

The band observed at 3890.9 cm^{-1} is consistent with a $2\nu_1$ overtone. For $Co^{12}C^{16}O$, $2\nu_1 = 2 \times 1957.5$ or 3915.0 cm^{-1}, which represents a X_{11} anharmonicity constant of -12.0 cm^{-1}. The $^{12}C/^{13}C$, $^{16}O/^{18}O$, and $^{12}C^{16}O/^{13}C^{18}O$ shifts for this overtone support this assignment, as the isotope shifts are very nearly twice those observed for the ν_1 fundamental (Table 1). From their positions and isotopic shifts, the weaker absorptions observed at 2534.9 and 2377.2 cm^{-1} for $Co^{12}C^{16}O$ are assigned to combination bands. Indeed, $\nu_1 + \nu_3 = 1957.5 + 579.2$ or 2536.7 cm^{-1} which represents a -1.8 cm^{-1} difference (X_{13}) with the band observed at 2534.9 cm^{-1}. The $^{12}C/^{13}C$, $^{16}O/^{18}O$, and $^{12}C^{16}O/^{13}C^{18}O$ shifts correlate well with the sum of the isotopic shifts observed for the fundamentals ν_1 and ν_3. Similarly, $\nu_1 + \nu_2 = 1957.5 + 424.9$ or 2382.4 cm^{-1} which represents a -5.2 cm^{-1} difference (X_{12}) with the band observed at 2377.2 cm^{-1}. Therefore this band has been assigned to $\nu_1 + \nu_2$. The isotopic shift with the $Co^{13}C^{16}O$ species correlate well with the sum of the isotopic shifts observed for the individual bands ν_1 and ν_3. From the anharmonicity corrections X_{11}, X_{12}, and X_{13}, one can derive consequently the harmonic frequency, ω_1, at 1989 ± 1 cm^{-1}, which can be used for comparison with theoretical prediction.

A harmonic force field calculation, using the Wilson's method,[17] was carried out using the experimental data presented in Table 1. More specifically, we searched for the set of harmonic force constants which would best reproduce the observed isotopic shifts for CoCO with the linear structure calculated in this study, i.e., $r_{CoC} = 1.673$ Å and $r_{CO} = 1.170$ Å. The best fit between the calculated harmonic frequencies for the various isotopic forms of CoCO and the experimental frequencies is presented in Table 4, with a 0.39% standard deviation. The force constants used in the calculation can be found in footnote *a* of Table 4. The simultaneous reproduction of all the isotope effects on the stretching modes imposes severe constraints on the form of the stretching normal coordinates, and the C−O, Co−C bonds, and interaction force constants are quite precisely determined. The differences observed between the calculated and experimental isotopic shifts for the ν_1 and ν_3 fundamentals are well within the realm of experimental uncertainties and of effects resulting from anharmonicity. For the ν_2 fundamental, however, the difference between calculated and experimental $^{12}C/^{13}C$, $^{16}O/^{18}O$, and $^{12}C^{16}O/^{13}C^{18}O$ isotopic shifts (+0.3, −1.1, and −0.8 cm^{-1}, respectively) are a little larger and vary from one isotopic species to the other in different directions, regardless of the absolute magnitude of the shift. Such a situation was already noted for PtCO,[18] PdCO,[19] and NiCO.[4] These small discrepancies cannot be explained by anharmonicity effects. Other geometries were also tested, but since any departure from linearity resulted in a larger standard deviation, the molecule will be taken as linear, in agreement with the theoretical predictions. The fit also improves globally with a larger r_{CoC}/r_{CO} ratio, but to obtain a difference between calculated and experimental isotopic shifts in the same direction, it is necessary to use unrealistic r_{CoC}/r_{CO} ratio (for example, 0.85), in view of the present theoretical results[3,6−8] (in fact, the calculated r_{CO} and r_{CoC} distances vary between 1.15 and 1.17 Å, and 1.65 and 1.71 Å, respectively, for the r_{CoC}/r_{CO} ratio of about 0.69).

It is interesting to note that a recent study of CO adsorption on Co(0001), using LEED technique, shows that the CO molecules adopt the on-top sites with the CO axis perpendicular to the surface. The measured value for the CO bond length is thus 1.17 ± 0.06 Å and for the Co−CO distance 1.78 ± 0.06 Å.[20] Also, at low coverage of CO on Co(10$\bar{1}$0), a C−O stretch at 1992 cm^{-1}, attributed to CO in on-top sites, was observed by reflection−absorption infrared spectroscopy (RAIRS) using 4 cm^{-1} resolution.[21] Finally, at high coverage of CO on Co-(10$\bar{1}$2), a Co−CO stretch at 440 cm^{-1}, attributed to CO in on-top sites, was observed by EELS spectroscopy using 95 cm^{-1} resolution.[22] From these vibrational surface values of CO in on-top sites on cobalt, it is interesting to determine the force constants F_{CO} and F_{Co-CO}. Using the simple Co−CO model with an infinite mass for the cobalt surface, we find 15.6 and 3.3 mdyn $Å^{-1}$, respectively. For the CoCO molecule, corresponding values were 14.74 and 3.96 mdyn $Å^{-1}$, respectively. The cobalt−CO bond force constant decreases from molecular to surface system (−17%), and the Co−C distance increases (1.67 and 1.78 Å, respectively). On the other hand, the CO bond force constant increases slightly (+6%), while the C−O distance is approximately the same (1.17 Å). In first approximation, these values are coherent with the relation between the bond length and the force constant.

Comparison with Other Metal−CO Molecules and Theoretical Predictions. The experimental vibrational frequencies and, for the ν_1, the harmonic frequency are presented in Table 2 along with values calculated with previous theoretical studies,[3,6−8] all with density functional theory (DFT), but with different functionals and/or basis sets. Of course the experimental values indicated here refer to CoCO isolated in solid argon and no attempt has been made to estimate the matrix shift, which for similar molecules reaches 2−3%, at most.[23−25] The position of the CoCO bending frequency ν_2 has been systemati-

TABLE 5: Comparison of Different Experimental Data for CoCO, NiCO, and CuCO

					vibrational frequencies (cm^{-1})		
	F_{MC} (mdyn Å^{-1})	F_{CO} (mdyn Å^{-1})	$F_{MC,CO}$ (mdyn Å^{-1})	F_{MCO} (mdyn Å rad^{-2})	ν_1	ν_2	ν_3
CoCO	3.96	14.74	0.55	0.468	1957.5	424.9	579.2
NiCO[a]	4.07	15.44	0.65	0.492	1994.5	409.1	591.1
CuCO[b]	1.02	16.58	0.52	0.141	2010.3	322.7	207.5

[a] Reference 4. [b] Reference 5.

cally underestimated in the calculations by 55, 105, 69, and 67 cm^{-1}(see Table 2), for a mean difference of 74 cm^{-1}(17%). This is a systematic situation for the linear MCO molecules (M= Ni, Pd, and Pt) already studied in this laboratory, for which no clear explanation for this situation has yet been proposed. It seems to be difficult to believe that the matrix effects shift so much the value of the bending mode.

For the Co−C stretching vibration, the calculated frequency of this study and with ref 3 are very good (+5 and +3%, respectively), and with ref 6 and ref 7, the calculated values are overestimated (+11%) and underestimated (−11%), respectively. For the C−O stretching vibration, the calculated values varied between 0.5 and 3%. We can conclude that the BP86 (refs 3 and 8) and the BPW91 (this study) functionals produce calculated frequencies in much better agreement with experiment. The calculated dissociation energy is higher with the BP86 (57.5 kcal/mol from ref 8) and the BPW91 (45 kcal/mol, this study) functionals, in comparison with the results of the others studies (30 and 26.8 kcal/mol). This is a relatively large difference, and unfortunately, no experimental determination of the dissociation energy of CoCO has yet been made. The predictions of IR intensities are successful as far as indicating approximate orders of magnitude between the very strong ν_1 mode and the other, weaker metal ligand vibrations, but the correct reproduction of IR intensities for the weaker fundamental seems a more challenging problem.

It is interesting to compare force constants obtained in the harmonic force field calculation for CoCO with those reported for NiCO and CuCO at the same level of approximation[4,5] (Table 5). The F_{CO} value decreases from CuCO to CoCO by about 11%, while the CO frequency decreases by only 2.6%, due to increased coupling between the M−C and C−O oscillators. The substitution of Ni by Co appears to weakly change the metal−CO bond force constant (F_{MC} = 4.07 and 3.96 mdyn Å^{-1}, respectively), but the change of Ni or Co to Cu appears to weaken this force constant (F_{CuC} =1.02 mdyn Å^{-1}). The interaction force constant between the M−C and C−O oscillators remains however very close in the three molecules ($F_{MC,CO}$ = 0.65, 0.52 and 0.55 mdyn Å^{-1} for NiCO, CuCO, and CoCO, respectively). Finally, the variation of the bending force constant is in the same direction as the variation of the metal−Co bond force constant, the molecule becoming progressively stiffer as the coordination bond is stronger.

Conclusions

The infrared absorption spectrum of cobalt monocarbonyl, synthesized by co-deposition of ground-state cobalt atoms and carbon monoxide molecules in solid argon and in situ electronic excitation of cobalt in the b ^{4}F state has been measured. Data obtained with $^{12}C/^{13}C$ and $^{16}O/^{18}O$ isotopes have enabled assignments of all fundamental vibrations and of three overtone and combination levels, and are analyzed with the help of semiempirical force field calculations. These results confirm that the CoCO molecule is linear while theoretical calculations on the Co + CO reaction give the molecular parameters of different states of the CoCO molecule and propose realistic reaction mechanisms to explain the formation of the CoCO molecule in its ($^2\Delta$) ground state and $^4\Phi$ and $^4A''$ first excited states.

References and Notes

(1) Hanlan, L. A.; Huber, H.; Kündig, E. P.; McGarvey, B. R.;. Ozin, G. A. *J. Am. Chem. Soc.* **1975**, *97*, 7054.
(2) Zhou, M.; Andrews, L. *J. Phys. Chem. A* **1998**, *102*, 10250.
(3) Zhou, M.; Andrews, L. *J. Phys. Chem. A* **1999**, *103*, 7773.
(4) Joly, H. A.; Manceron, L. *Chem. Phys.* **1998**, *226*, 61.
(5) Tremblay, B.; Manceron, L. *Chem. Phys.* **1999**, *242*, 235.
(6) Fournier, R. *J. Chem. Phys.***1993**, *99*, 1801.
(7) Adamo, C.; Lelj, F. *J. Chem. Phys.* **1995**, *103*, 10605.
(8) Ryeng, H.; Gropen, O.; Swang, O. *J. Phys. Chem. A* **1997**, *101*, 8956.
(9) Sugar, J.; Corliss, C. *J. Phys. Chem. Ref. Data Suppl. No. 2* **1985**.
(10) Bishop, D. M.; Cheung, L. M. *J. Phys. Chem. Ref. Data* **1982**, *11*, 121.
(11) Frisch, M. J.; Trucks, G. W.; Schlegel, H. B.; Scuseria, G. E.; Robb, M. A.; Cheeseman, J. R.; Zakrzewski, V. G.; Montgomery, J. A., Jr.; Stratmann, R. E.: Burant, J. C.; Dapprich, S.; Millam, J. M.; Daniels, A. D.; Kudin, K. N.; Strain, M. C.; Farkas, O.; Tomasi, J.; Barone, V.; Cossi, M.; Cammi, R.; Menniccu, B.; Pomelli, C.; Adamo, C.; Clifford, S.; Ochterski, J.; Petersson, G. A.; Ayala, P.Y.; Cui, Q.; Morokuma, K.; Malick, D. K.; Rabuk, A. D.; Raghavachari, K.; Foresman, J. B.; Cioslowski, J.; Ortiz, J. V.; Baboul, A. G.; Stefanov, B. B.; Liu, G.; Liashenko, A.; Piskorz, P.; Komaromi, I.; Gomperts, R.; Martin, R. L.; Fox, D. J.; Keith, T.; Al-Laham, M. A.; Peng, C. Y.; Nanayakkara, A.; Challacombe, M.; Gill, P. M. W.; Johnson, B.; Chen, W.; Wong, M. W.; Andres, J. L.; Gonzalez, C.; Head-Gordon, M.; Replogle, E. S.; Pople, J. A.; *Gaussian 98, Revision A.9*; Gaussian, Inc.: Pittsburgh, PA, 1998.
(12) Becke, A. D. *Phys. Rev. A* **1988**, *38*, 3098.
(13) Perdew, J. P.; Wang, Y. *Phys. Rev. B* **1992**, *45*, 13244.
(14) McLean, A. D.; Chandler, G. S. *J. Chem. Phys.* **1980**, *72*, 5639.
(15) Krishnan, R.; Binkley, J. S.; Seeger, R.; Pople, J. A. *J. Chem. Phys.* **1980**, *72*, 650.
(16) Shaefer, A.; Huber, C.; Ahlrichs, R. *J. Chem. Phys.* **1994**, *100*, 5829.
(17) Wilson, E. B., Jr.; Decius, J. C.; Cross, P. C. *Molecular Vibrations*; Mc-Graw-Hill: New York, 1955; Dover Publications: New York, 1980; pp 303−306.
(18) Manceron, L.; Tremblay, B.; Alikhani, M. E. *J. Phys. Chem. A* **2000**, *104*, 3750.
(19) Tremblay, B.; Manceron, L. *Chem. Phys.* **1999**, *250*, 187.
(20) Lahtinen, J.; Vaari, J.; Kauraala, K.; Soares, E. A.; Van Hove, M. A. *Surf. Sci.* **2000**, *448*, 269.
(21) Toomes, R. L.; King, D. A. *Surf. Sci.* **1996**, *349*, 1.
(22) Geerlings, J. J. C.; Zonnevylle, M. C.; de Groot, C. P. M. *Surf. Sci.* **1991**, *241*, 315.
(23) Jacox, M. E. *Chem. Phys.* **1994**, *189*, 149.
(24) Tanaka, K.; Tachikawa, Y.; Tanaka, T. *J. Chem. Phys.* **1997**, *106*, 2118.
(25) Zhou, M. F.; Chertihin, G. V.; Andrews, L. *J. Chem. Phys.* **1998**, *109*, 10893.